Lamb mode spectra versus the Poisson ratio in a free isotropic elastic plate

Daniel Royer, Dominique Clorennec, and Claire Prada
Laboratoire Ondes et Acoustique, ESPCI, Université Paris 7, CNRS UMR 7587, 10 rue Vauquelin, 75231 Paris Cedex 05, France

(Received 23 December 2008; revised 20 March 2009; accepted 20 March 2009)

The variation, with material parameters, of Lamb modes is investigated. Vibration spectra of traction-free elastic plates are generally presented, for a given isotropic material, as a set of dispersion curves corresponding to the various Lamb mode branches. Here, the spectrum variations, with the Poisson ratio ν, are plotted in a dimensionless co-ordinate system in the form of a bundle of curves for each Lamb mode. Except for the fundamental anti-symmetric mode A_0, this representation highlights the same behavior for all Lamb modes. V_T denoting the shear wave velocity, the (ω,k) plane can be divided into two angular sectors separated by the line of slope $V_T\sqrt{2}$. In the upper one, corresponding to a phase velocity $V=\omega/k$ larger than $V_T\sqrt{2}$, dispersion curves are very sensitive to the plate material parameters. In the lower sector $(V<V_T\sqrt{2})$ all the branches, whatever the value of the Poisson ratio $(0\leq\nu<0.5)$, are gathered into a thin pencil. Moreover, curves of a given bundle cross the boundary line at coincidence points equally spaced. These properties and a specific behavior observed for $\nu=0$ are explained in terms of Lamé wave solutions of the characteristic equations of Lamb modes.
 [DOI: 10.1121/1.3117685]

PACS number(s): 43.40.Dx, 43.20.Mv [YHB] Pages: 3683–3687

I. INTRODUCTION

The characteristic equations governing the propagation of symmetric (S_n) and anti-symmetric (A_n) modes in a free isotropic plate was derived by Rayleigh.[1] First numerical solutions were obtained for the phase velocity V of the lowest modes by Lamb.[2] The propagation of these guided waves can be represented by a set of dispersion curves giving the angular frequency $\omega=2\pi f$ of each modes versus the wave number $k=2\pi/\lambda$. Plots of dispersion curves, numerically calculated for various materials, can be found in many textbooks.[3–6] They show the complexity of Lamb waves frequency spectra as a result of the coupling of shear waves (velocity V_T) and longitudinal waves (velocity V_L) at the traction-free surfaces.

Before the extensive use of computers, crossings of Lamb mode branches were investigated as a guide for sketching Lamb wave spectra without numerical calculations. Due to mode orthogonality,[7] curves of the same family never intersect. Crossing points between symmetric and anti-symmetric curves were first studied by Mindlin.[8] This author developed a method based on mixed boundary conditions for which shear and dilatational waves are uncoupled. The grid of intersecting dispersion curves for a plate subjected to these artificial boundary conditions forms a series of bounds for the dispersion curves of Lamb modes. Using dimensionless variables, Lamb wave frequency spectra only depend on the bulk wave velocity ratio V_L/V_T or Poisson's ratio ν. Extending Mindlin's method, Freedman[9] studied the variation of Lamb mode spectra over the full range of Poisson's ratio $(-1<\nu<0.5)$. This author also showed that coincidences of branches of like symmetry modes occur at intersection of bounds and for a ratio of the wave number k to the shear wave number in the plate material $(k_T=\omega/V_T)$ equal to $2^{-1/2}$. In a companion paper,[10] the special behavior of Lamb modes at $\nu=0$ was investigated in terms of Mindlin rules. In a third paper,[11] Freedman examined the variation of individual branches of lower order Lamb modes over the complete range of Poisson ratio.

In Freedman's papers, the dispersion curves are generally presented on an unusual plot of k/k_T versus d/λ_T (d denoting the plate thickness) and figures are schematic illustrations of the variations of Lamb branches. Additionally, a large number of accurate frequency spectra can be found in the literature on Lamb waves. However, each spectrum, computed for a given material or a fixed value of the Poisson ratio, is composed of many branches corresponding to various modes. From the juxtaposition of these families of dispersion curves, it is not easy to conclude on the evolution of Lamb modes with the mechanical properties of the plate material. It is thus desirable to reach a clear insight on the variations of the lower order Lamb mode branches with material parameters.

The objective of the present paper is to clarify the manner in which the frequency spectrum of Lamb waves varies with the Poisson ratio. For this purpose, the dispersion curves are presented in a co-ordinate system giving the normalized frequency $F=fd/V_T$ versus the normalized wave number $K=kd/2\pi=d/\lambda$. Moreover, we present the spectrum in the form of a bundle of curves for a selected Lamb mode. These plots show general trends and clearly highlight the specific behavior of Lamb modes at points where they consist solely of shear waves propagating at 45° to the plate surfaces.

II. NUMERICAL RESULTS

In a homogeneous isotropic plate, Lamb waves are either symmetric or anti-symmetric. For each family the angular frequency and the wave number satisfy a characteristic or frequency equation.[3] When the faces of the plate are free of tractions, no energy leakage occurs. Then, for any real k, the secular equation yields an infinite number of real roots in ω. The dispersion curves of these propagating modes, guided by the plate, is represented by a set of branches in the (ω,k) plane. Many frequency spectra can be found in the literature. Each of them, computed for a given material, testifies the complexity of Lamb wave propagation.

Elastic properties of an isotropic material are characterized by two constants c_{11} and c_{66}, related to longitudinal and shear wave velocities, respectively, V_L and V_T. The use of dimensionless frequency $F=fd/V_T$ and wave number $K=kd/2\pi$ allows us to express Lamb wave propagation in terms of only one material parameter, the bulk wave velocity ratio $\kappa=V_L/V_T$ or the Poisson ratio ν:

$$\nu=\frac{\kappa^2-2}{2(\kappa^2-1)} \tag{1}$$

and

$$\kappa=\frac{V_L}{V_T}=\sqrt{\frac{2(1-\nu)}{1-2\nu}}. \tag{2}$$

The advantage of Poisson's ratio is that this coefficient remains finite. With very few special exceptions, isotropic materials exhibit positive Poisson ratio. Therefore, the study is limited to the usual range, i.e., from the rigid solid ($\nu=0 \rightarrow \kappa=\sqrt{2}$) to the fluid ($\nu=0.5 \rightarrow \kappa=\infty$).

Numerical calculations have been performed in order to determine the normalized frequency F versus normalized wave number K. Dispersion curves were plotted for $0\leq K\leq 5$ and $0\leq F\leq 6$ and for 11 values of the Poisson ratio ν from 0 to 0.49. The first ten values are separated by a step equal to 0.05. The limiting case of a fluid, with $V_T=0$ and $\nu=0.5$, is not considered here. Results are presented in Fig. 1 for the first four anti-symmetric modes and in Fig. 2 for the first four symmetric modes. In these graphs, a straight line of unit slope corresponds to a phase velocity $V=\omega/k$ equal to V_T. This representation highlights some conclusions on the behavior of Lamb modes versus the plate material properties.

For a given mode, the lower curve of a bundle corresponds to $\nu=0$ and the upper one to $\nu=0.49$. This continuous evolution of the frequency spectrum observed for all the Lamb modes can be easily explained. Equation (2) shows that the bulk wave velocity ratio $\kappa=V_L/V_T$ increases with the Poisson ratio. Thus, in a co-ordinate system where the frequency thickness product is normalized to the shear wave velocity V_T, the dispersion curves are pulled toward high normalized frequencies when the longitudinal wave velocity V_L increases.

Except for the fundamental anti-symmetric mode A_0, the (ω,k) plane can be divided in two angular sectors. In the upper sector, corresponding to a phase velocity $V=\omega/k$ larger than $V_T\sqrt{2}$, dispersion curves are very sensitive to the material parameters. In the lower sector ($V<V_T\sqrt{2}$) all the

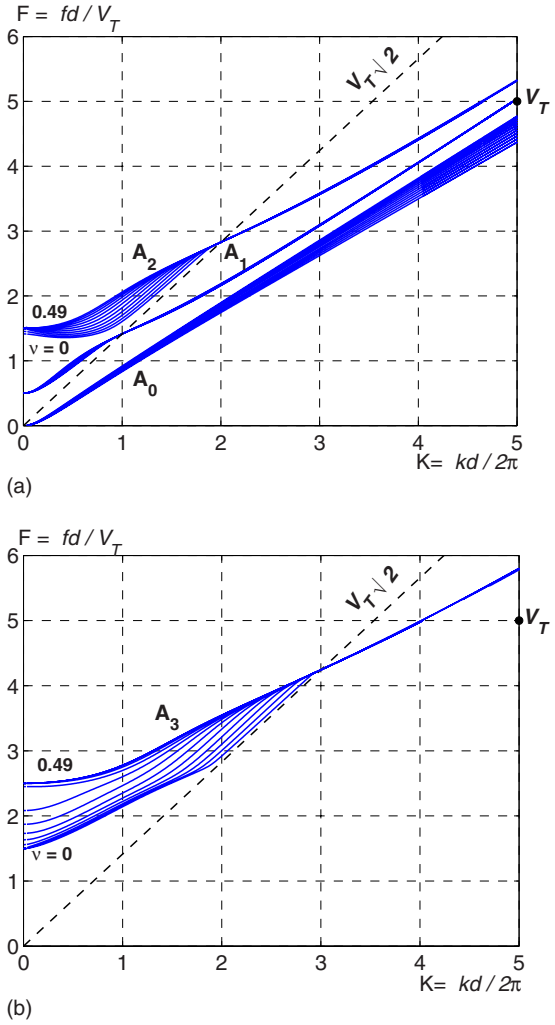

FIG. 1. (Color online) Variation, with Poisson's ratio in the range $0\leq\nu\leq 0.49$, of anti-symmetric Lamb modes in an isotropic free plate of thickness d. Bundle of dispersion curves for (a) A_0, A_1, and A_2 modes, and (b) A_3 mode. For each mode, the lower curve corresponds to $\nu=0$ and the upper one to $\nu=0.49$.

curves, whatever the value of Poisson's ratio, are gathered into a thin pencil. It should be noted that this velocity $(V_T\sqrt{2})$ represents the lowest possible value of the longitudinal bulk wave velocity V_L reached at zero Poisson ratio. Thus in the lower sector, for any material, the phase velocity is smaller than V_L, which dramatically reduces the influence of bulk wave velocity ratio and Poisson ratio on Lamb mode dispersion curves. For large values of kd, i.e., $d\gg\lambda$, the non-zero order symmetric and anti-symmetric branches tend asymptotically toward a unit slope, corresponding to a phase velocity equal to V_T. Lamb modes are often used to characterize material properties in platelike structures.[12] This remark indicates that for high order modes $(n\geq 1)$ the sensitivity to material parameter ν or $\kappa=V_L/V_T$ is much larger in the upper sector.

Branches of a given Lamb mode cross the line corresponding to the phase velocity $V_T\sqrt{2}$ at a fixed point independent of the Poisson ratio. These points are equally spaced on this line and their abscissa kd are equal to $(2n+1)\pi$ for the symmetric mode S_n $(K=n+1/2)$ and $2n\pi$ for the anti-symmetric mode A_n $(K=n)$, respectively. Curves of a given

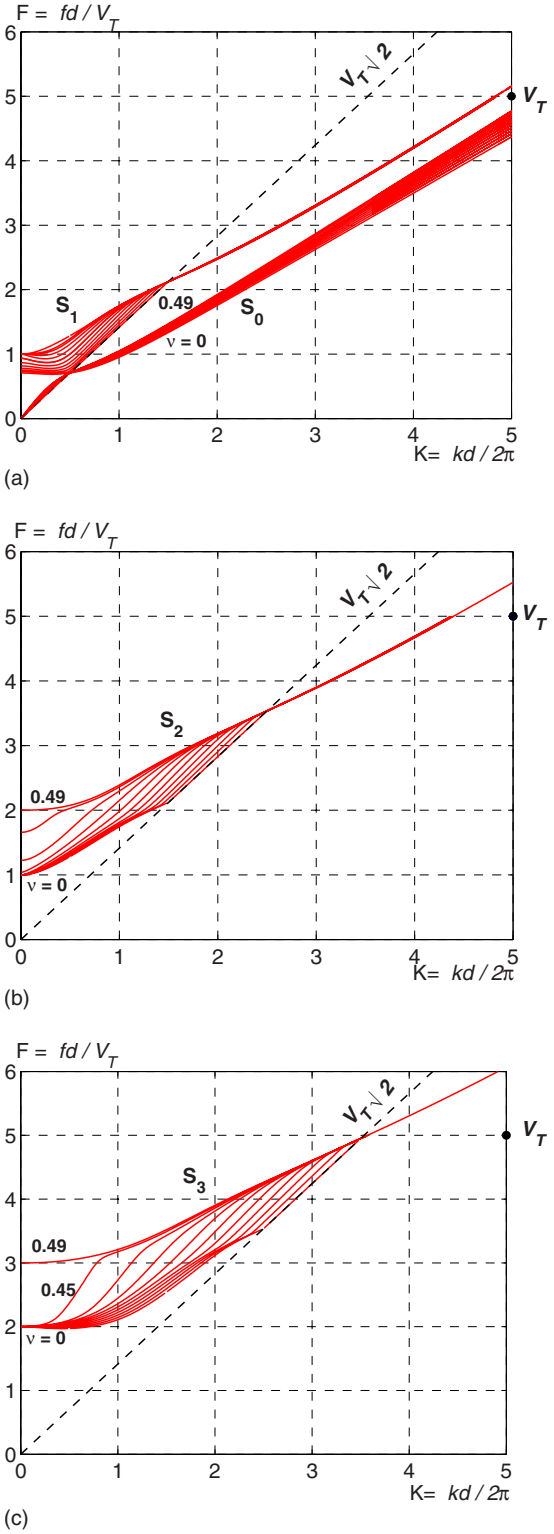

FIG. 2. (Color online) Variation, with Poisson's ratio in the range $0 \leqslant \nu \leqslant 0.49$, of symmetric Lamb modes in an isotropic free plate of thickness d. Bundle of dispersion curves for (a) S_0 and S_1 modes, (b) S_2 mode, and (c) S_3 mode. For each mode, the lower curve corresponds to $\nu=0$ and the upper one to $\nu=0.49$.

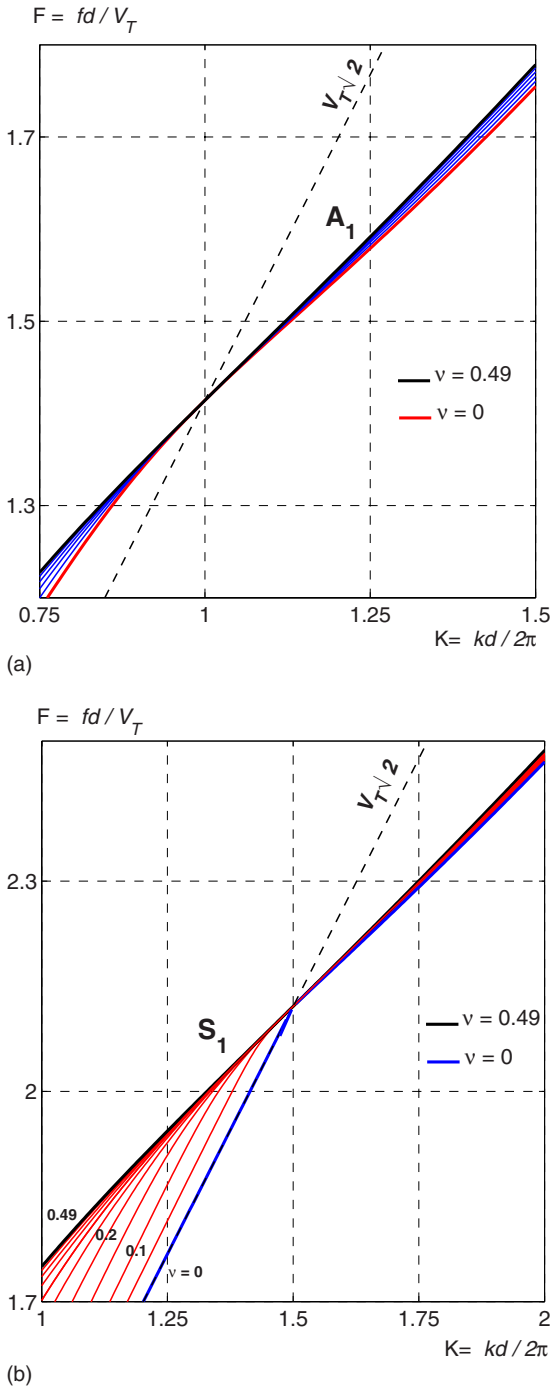

FIG. 3. (Color online) Behavior of dispersion curves over the coincidence points. (a) A_1 mode and (b) S_1 mode. Dispersion curves of a given mode cross the line $F=\sqrt{2}K$ with the same slope.

bundle do not intersect each other. Figure 3 illustrates this behavior for modes A_1 and S_1, showing that dispersion curves cross the line $F=\sqrt{2}K$ at the common point with the same slope. All branches of a bundle pass through the line so tangentially that their order does not change at the coincidence point. This property is valid for all the symmetric and anti-symmetric modes.

In the case of a rigid solid ($\nu=0$), Fig. 4(a) shows that symmetric Lamb modes exhibit a particular behavior. It appears that all the segments of the line $F=\sqrt{2}K$ belong to successive symmetric modes. The change from mode S_n to mode S_{n+1} occurs at the coincidence point of abscissa $kd=(2n+1)\pi$, giving rise to a discontinuity of the slope and thus of the group velocity $V_g=d\omega/dk$. These remarks are not valid for the anti-symmetric modes [Fig. 4(b)].

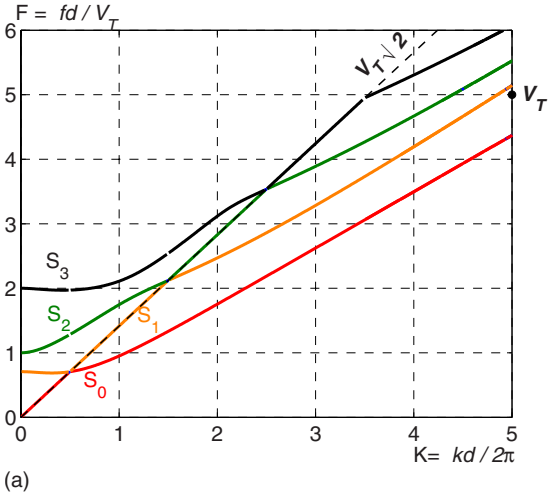

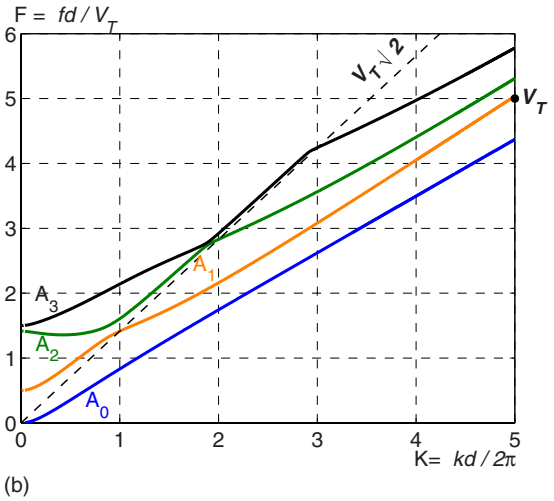

FIG. 4. (Color online) Special behavior at $\nu=0$ (rigid solid). (a) Symmetric Lamb modes: segments of the Lamé line belong to successive modes. The change from mode S_n to mode S_{n+1} occurs at the coincidence point of abscissa $K=n+1/2$ and gives rise to a discontinuity of the slope. (b) This discontinuous behavior is not observed on anti-symmetric branches.

In the following part, most of the features observed on Lamb mode frequency spectra are explained from the specific conditions for which the modes propagating in the free isotropic plate are Lamé modes, consisting solely of shear waves, or a degenerate Lamé mode, consisting of a purely longitudinal wave.[13]

III. INTERPRETATION IN TERMS OF LAMÉ MODES

The characteristic equations of Lamb modes result from the traction-free boundary conditions on the surfaces, located at $x_2=\pm h$ for a plate of thickness $d=2h$. Using classical notations:[5,6]

$$q^2=k_T^2-k^2 \quad \text{and} \quad p^2=k_L^2-k^2, \tag{3}$$

boundary conditions may be expressed, for the symmetric modes ($\alpha=0$) and the anti-symmetric modes ($\alpha=\pi/2$), as

$$(k^2-q^2)B\cos(ph+\alpha)+2ikqA\cos(qh+\alpha)=0 \tag{4}$$

and

$$2ikpB\sin(ph+\alpha)+(k^2-q^2)A\sin(qh+\alpha)=0. \tag{5}$$

A and B are the amplitudes of the vector and scalar displacement potentials, respectively.

Lamé modes are particular solutions of these equations for $k_T^2=2k^2$, i.e., for a phase velocity V equal to $V_T\sqrt{2}$. With

$$q^2=k^2 \quad \text{and} \quad p^2=-\frac{\nu}{1-\nu}k^2, \tag{6}$$

boundary conditions are satisfied with $kh=(n+1/2)\pi$ for the symmetric modes ($\alpha=0$) and $kh=n\pi$ for the anti-symmetric modes ($\alpha=\pi/2$). In both cases the amplitude B of the scalar potential vanishes, giving rise to a pure shear wave reflecting at 45° on the plate boundaries for which no mode conversion into longitudinal waves occurs.[14] The resulting guided wave propagates along the axis of the plate at the phase velocity $V=V_T\sqrt{2}$. These solutions exist for any positive value of ν and the normalized co-ordinates of their representative points are the equally spaced values:

$$K=m/2 \quad \text{and} \quad F=m/\sqrt{2}, \tag{7}$$

where m is an odd (even) integer for the symmetric (anti-symmetric) modes. Moreover, the acoustic energy is carried at a velocity equal to the projection of the shear wave velocity on the plate axis. Thus, the group velocity $V_g=d\omega/dk$ of Lamé modes is equal to $V_T/\sqrt{2}$, i.e., half the phase velocity.

Since positions and slopes of Lamé modes are independent of the Poisson ratio, each Lamb mode of a given bundle passes through the Lamé line $F=\sqrt{2}K$ at the same point with the same slope. This behavior is observed in Figs. 1 and 2 for all the Lamb modes, except for the anti-symmetrical mode A_0 whose phase velocity is less than the Rayleigh wave velocity V_R, thus less than V_T.

For the special case $\nu=0\rightarrow p=0$ and for the symmetric modes, another solution of Eqs. (4) and (5) exists with $A=0$ and a non-zero scalar potential ($B\neq 0$). In a rigid solid, the Lamé solutions correspond to a constant longitudinal displacement propagating at the velocity $V_L=V_T\sqrt{2}$. Conversely to the non-degenerate Lamé modes, the boundary conditions are satisfied for any wave number k. Thus, as shown in Fig. 4(a), the Lamé line is a locus for the roots of the Rayleigh–Lamb equation. Segments of the Lamé line belongs to successive symmetric modes, the change from modes S_n to S_{n+1} occurring at the coincidence point of abscissa $kd=(2n+1)\pi$. At this point, the S_n branch changes direction giving rise to a discontinuity of the group velocity from $V_T\sqrt{2}$ to $V_T/\sqrt{2}$. The inverse change occurs for the mode S_{n+1}. As predicted, Fig. 4(b) shows that this behavior is specific to symmetric modes.

IV. CONCLUSION

Although the propagation of elastic waves in an isotropic plate has been widely investigated, the influence of plate material properties on Lamb mode spectra was not easy to derive from the uncountable frequency spectra found in the literature. Using a dimensionless co-ordinate system, the way individual Lamb mode branches vary with the Poisson ratio ν was investigated. A representation in the form of a bundle of dispersion curves shows that the normalized frequency

increases continuously with the Poisson ratio and also highlights some feature common for all Lamb modes, except for the fundamental anti-symmetric one A_0. The (ω,k) plane can be divided in two angular sectors separated by a line of slope equal to the phase velocity $V_T\sqrt{2}$ of the Lamé modes. In the upper one, corresponding to a phase velocity V larger than $V_T\sqrt{2}$, the frequency spectrum is very sensitive to Poisson's ratio. In the lower sector $(V<V_T\sqrt{2})$, all curves in a bundle are gathered into a thin pencil, with a weak dependence on Poisson's ratio. Moreover, all the dispersion curves of a given Lamb mode cross the boundary line at a fixed point with the same slope. These coincidence points are equally spaced: their abscissa are such that $kd=2n\pi$ for the anti-symmetric mode A_n and $kd=(2n+1)\pi$ for the symmetric mode S_n. In the case of a rigid solid $(\nu=0)$, a specific behavior is observed: segments of the Lamé line belong to successive symmetric modes. The change from modes S_n to S_{n+1} occurs at the coincidence point of abscissa $kd=(2n+1)\pi$.

[1]Lord Rayleigh, "On the free vibrations of an infinite plate of homogeneous isotropic elastic matter," Proc. London Math. Soc. **20**, 225–234 (1889).
[2]H. Lamb, "On waves in an elastic plate," Proc. R. Soc. London, Ser. A **93**, 114–128 (1917).
[3]I. A. Viktorov, *Rayleigh and Lamb Waves: Physical Theory and Applications* (Plenum, New York, 1967).
[4]B. Auld, *Acoustic Fields and Waves in Solids II* (Wiley Interscience, New York, 1973).
[5]J. D. Achenbach, *Wave Propagation in Elastic Solids* (North-Holland, Amsterdam, 1980).
[6]D. Royer and E. Dieulesaint, *Elastic Waves in Solids 1: Free and Guided Propagation* (Springer, Berlin, 1999).
[7]W. B. Fraser, "Orthogonality relation for the Rayleigh–Lamb modes of vibration of a plate," J. Acoust. Soc. Am. **59**, 215–216 (1976).
[8]R. D. Mindlin, "Mathematical theory of vibrations of elastic plates," in Proceedings of 11th Annual Symposium on Frequency Control (U.S. Army Signal Engineering Laboratories, Fort Monmouth, NJ, 1957), pp. 1–40.
[9]A. Freedman, "The variation, with the Poisson ratio, of Lamb modes in a free plate, I: General spectra," J. Sound Vib. **137**, 209–230 (1990).
[10]A. Freedman, "The variation, with the Poisson ratio, of Lamb modes in a free plate, II: At transitions and coincidence values," J. Sound Vib. **137**, 231–247 (1990).
[11]A. Freedman, "The variation, with the Poisson ratio, of Lamb modes in a free plate, III: Behaviour of individual modes," J. Sound Vib. **137**, 249–266 (1990).
[12]W. Gao, C. Glorieux, and J. Thoen, "Laser ultrasonic study of Lamb waves: Determination of the thickness and velocities of a thin plate," Int. J. Eng. Sci. **41**, 219–228 (2003).
[13]V. Pagneux, "Revisiting the edge resonance for lamb waves in a semi-infinite plate," J. Acoust. Soc. Am. **120**, 649–656 (2006).
[14]*Elastic Waves in Solids 1: Free and Guided Propagation* (in Ref. 6), p. 321.